Accepted Manuscript

Raman study of light-emitting SiN$_x$ films grown on Si by low-pressure chemical vapor deposition

F. Komarov, L. Vlasukova, I. Parkhomenko, O. Milchanin, A. Mudryi, A. Togambaeva, O. Korolik

Raman study of light-emitting SiN$_x$ films grown on Si by low-pressure chemical vapor deposition

F. Komarov [a], L. Vlasukova [b], I. Parkhomenko [b*)], O. Milchanin [a], A. Mudryi [c],

A. Togambaeva [d], O. Korolik [b]

[a] *A.N. Sevchenko Institute of Applied physics problems, Kurchatov Str. 7, 220045, Minsk, Belarus*

[b]*Belarusian State University, Nezavisimosty Ave. 4, 220030, Minsk, Belarus*

[c]*Scientific and Practical Materials Research Center, National Academy of Sciences of Belarus, P. Brovki Str. 17, 220072, Minsk, Belarus*

[d]*Al-Farabi Kazakh National University, Al-Farabiy Ave. 71, 050038, Almaty, Kazakhstan*

Corresponding author: [*)] Tel.: +375 17 209 59 29; fax: +375 17 212 48 33

E-mail address: irinaparkhomen@gmail.com (Irina Parkhomenko)

ABSTRACT

Si-rich silicon nitride (SRSN) films were deposited on Si wafers by low pressure chemical vapor deposition (LPCVD) technique and, subsequently, annealed at (800 – 1200) °C to form Si precipitates. The composition of SiN$_x$ films was measured by Rutherford backscattering spectrometry (RBS). Two sets of samples differed by the amount of excessive Si (Si$_{exc}$) in silicon nitride were studied. Evolution of Si nanoclusters from amorphous to crystalline ones during high temperature treatment was examined by Raman scattering (RS) spectroscopy. The amorphous Si clusters were already revealed in as-deposited SiN$_x$ while the annealing results in their crystallization. The crystalline nanoprecipitates are only registered in nitride films after annealing at 1200 °C. A dependence of Raman scattering intensity from the Si wafer on the temperature of annealing of SiN$_x$/Si structures was revealed. This information was used to explain the phase transformations in SRSNs during high temperature treatments. The peculiarities of photoluminescence (PL) spectra for two sets of Si-rich SiN$_x$ films are explained

taking into account the contribution from the quantum confinement effect of Si nanocrystals and from the native defects in silicon nitride matrix, such as N- and K- centers.

1. Introduction

Over the past two decades, a quantum confinement effect in silicon-based nanostructures is of great interest because of its potential for promoting the integration of optoelectronic devices with silicon very large scale integration technology. A variety of techniques has been exploited to obtain low-dimensional silicon structures, such as silicon nanocrystals (Si-NCs) synthesized by ion implantation [1-2], sputtering [3], and plasma-enhanced chemical vapor deposition (PECVD) [4-6], silicon nanopillars and nanowires formed by dry etch [7-8] and chemical sythesis [9-10]. Initially, efforts of researchers were focused on the light emission of Si-NCs embedded in silicon oxide matrix. However, it has been found out that Si-NCs would have unsatisfactory electroluminescence characteristics due to the difficulty of carrier tunneling through a wide energy bandgap of silicon oxide matrix [10-11]. Theoretical and experimental investigations predict a high potential barrier ($\approx$ 8.5 eV) for silicon oxide with silicon nanocrystals [12]. Silicon nitride films with Si-NCs provide a lower barrier ($\approx$ 2.0 eV) for carriers and more intense light emission than those of silicon oxide [13]. That is why, silicon nitride has been considered as a preferable matrix material for preparation of Si-NCs-related devices.

Strong visible photo- and electroluminescence from SiN_x films with Si-NCs, also tunable by adjusting the silicon content, has been widely reported with different interpretations [14-25]. However, the origin of the luminescence is still an object of controversy, primarily due to a lack of distinction between luminescence originating from silicon precipitates and from silicon nitride matrix. Often, a visible luminescence is explained by quantum confinement effect of crystalline [17, 20, 26-27] or amorphous [16] Si-NCs. In other cases, the luminescence has been ascribed to

defect states [28-29], surface states at the nanoparticle–matrix interface [30], or radiative recombination between localized band-tail states [18-19].

A number of researchers reported on visible PL of silicon nitrides fabricated via PECVD. Such SiN_x films contain a large concentration up to (20 - 40%) of hydrogen because of using hydrogen-containing gases (silane and ammonia) and low temperature of deposition ($\leq$ 350 °C) [31]. It is known that hydrogen atoms incorporated in nitride matrix influence on the structural and optical properties of silicon nitride films [32]. In order to distinguish the mechanisms of silicon nitride luminescence, it is important to investigate the structural and light-emitting properties of hydrogen-free SiN_x films. For fabrication of such structures, low-pressure chemical vapor deposition (LPCVD) can be considered as a preferable technique, as it is conducted at high deposition temperatures (near to 800 °C) and enables us to prepare SiN_x films with a negligible hydrogen concentration.

Taking into account that Si-NCs quantum confinement effect may contribute in resulting SiN_x luminescence, it is important to estimate an average size of nanoclusters and to clear up the question if Si nanoclusters in SiN_x matrix are amorphous or crystalline quantum dots. In comparison with amorphous nanoclusters, the nanocrystals are more preferable for device applications for the following reasons [33]:

–amorphous state is metastable, so the device parameters can be subjected to degradation;

–usually, the rate of nonradiative transitions in crystalline clusters is lower than that in the amorphous clusters, so the PL intensity for nanocrystals is, generally, higher than that for amorphous nanoclusters.

In comparison with conventional methods to study nanomaterials and nanostructures, such as transmission electron microscopy and X-ray diffraction, micro-Raman scattering spectroscopy is much preferred for its nondestructive measuring, small specimen quantity and short measurement time. Moreover, a line shape analysis of the first-order Raman spectrum provides

with the information on the average size of nanoprecipitates as well as crystalline or amorphous nature of the material [34].

The aim of this paper is to study phase transformations (formation and crystallization of Si clusters) in LPCVD - Si-rich SiN_x films during the high temperature treatment and to reveal a correlation between these transformations and PL of nitride films.

2. Experimental details

The SRSN films were deposited on n-type (100)-oriented Si substrates by low pressure chemical vapor deposition at 800 °C using the gaseous mixture of dichlorosilane (SiH_2Cl_2) and ammonia (NH_3) as precursors. The thickness and refractive index of nitride films were measured by laser ellipsometry at λ=632.8 nm. Two SiN_x/Si wafers (labeled hereafter as $SiN_{0.46}$ and $SiN_{1.0}$) were fabricated. The samples with the size of 1×1 cm^2 were cut out of $SiN_{0.46}$ and $SiN_{1.0}$ wafers and annealed in nitrogen ambient at 800 °C and 1000 °C during 60 min in a resistance furnace and at 1200 °C during 3 min using the rapid thermal annealing setup 'jetFirst'. The composition of as-deposited SiN_x films was determined by Rutherford backscattering spectrometry using 1.3 MeV He^+ ions from HVE accelerator. The amount of excessive silicon Si_{exc} was calculated by the following equation [35]:

$$Si_{exc.} = \frac{Si_{at.\%}}{Si_{at.\%}+N_{at.\%}} - \frac{3}{7}. \quad (1)$$

The structural properties of Si nanoclusters in SRSN films were studied using Raman scattering technique on both as-deposited and annealed samples. RS measurements were carried out by micro-Raman setup Nanofinder. The samples were excited with a laser beam (λ = 473 nm) and the scattered light was detected in back-scattering geometry at room temperature. PL spectra were recorded at room temperature in the spectral region of 350 – 800 nm using a He-Cd laser source with λ= 325 nm.

3. Results and discussion

The values of thickness, refractive index, stoichiometric parameter x and amount of excessive Si in SiN_x for the as-deposited films $SiN_{0.46}$ and $SiN_{1.0}$ are summarized in Table 1.

As shown in Table 1, the same refractive index and similar thickness are recorded for $SiN_{0.46}$ and $SiN_{1.0}$ samples. Refractive index n was used by some authors in order to evaluate the stoichiometric parameter x of SiN_x films [16]. The $SiN_{1.33}$ composition is believed to be characterized with n between 1.8 and 2.0 depending on the growth procedure. The SRSN with stoichiometric parameter $x < 1.3$ is characterized with $n > 2.0$. The more excessive (over stoichiometric) Si atoms are incorporated in SRSN films, the more high value of n is associated to them [36]. Nevertheless, in our experiment the RBS data reveal that two samples with the same n, $SiN_{0.46}$ and $SiN_{1.0}$, differ by the total quantity of excessive Si. It can be explained as follows. The optical constants of SiN_x layers are determined not only by the value of x, which depends on the concentration of excessive Si atoms, but also on the spatial localization of these excessive atoms. The excessive silicon can be randomly distributed over the atomic network or aggregated in clusters of different sizes in the SiN_x matrix [37].

To confirm the trends, we also performed RS experiments on these samples. *Fig 1* shows the Raman spectra of the as-deposited and annealed at (800 – 1200 °C) samples $SiN_{0.46}$ and $SiN_{1.0}$. All samples exhibit the narrow peak at 520 cm^{-1}. It arises from the light scattering by the Si (100) substrate. The spectra of as-deposited $SiN_{0.46}$ and $SiN_{1.0}$ samples contain also a broad band at 480 cm^{-1}. This band is attributed to amorphous silicon [38]. Thus, we can conclude that there are amorphous silicon clusters in both as-deposited samples ($SiN_{0.46}$ and $SiN_{1.0}$). A partially phase-separated structure, constituted by a mixture of a silicon reach phase and a phase containing more nitrogen atoms is then plausible.

The analysis of RS spectra transformation after the annealing reveals two similar features for the both sets of samples. Firstly, when increasing the annealing temperature, the band at 480 cm^{-1} disappeared and a low-energy tail of the band at 520 cm^{-1} was observed. This low-energy tail can be assigned to the light scattering from silicon nanocrystals. It should be noted

that similar modifications of Raman spectra were observed in Ref [39] for Si-rich silicon oxide films with embedded Si nanoparticles. In this paper, the spectra of the SiO_x films annealed at 1300 K for 60 min exhibit two obvious components. The sharp peak at 520 cm^{-1} was assigned to the silicon substrate, and the low-energy tail was due to the Si nanocrystals. The presence of Si nanocrystals was confirmed by high resolution electron microscopy [39].

Thus, the spectral transformations, manifested in *Fig. 1*, can be assigned to the crystallization of amorphous clusters in the films. It should be noted that in the case of $SiN_{1.0}$ sample, the low-energy tail is observed after the annealing at lower temperature (1000 °C) in comparison with the $SiN_{0.46}$ sample. Regarding the sample $SiN_{0.46}$, the band at 480 cm^{-1} disappears, and a weak low-energy tail appears only after annealing at 1200 °C. Therefore, one can conclude that the temperature of the beginning of amorphous clusters crystallization is different for the samples $SiN_{0.46}$ and $SiN_{1.0}$. It can be caused by the difference between an average size of initial amorphous clusters embedded in the as-deposited films $SiN_{0.46}$ and $SiN_{1.0}$. Size-dependent crystallization of silicon nanoprecipitates was studied by RS spectroscopy in Ref. [40]. According to their observation, the threshold temperature of the amorphous/crystalline transition for silicon nanoclusters decreases as the particle size decreases. Thus, one can conclude that the average size of silicon clusters in the $SiN_{0.46}$ sample exceeds that in the $SiN_{1.0}$ sample. It does not contradict the higher excess of silicon content in the sample $SiN_{0.46}$.

Secondly, a similar feature of the RS spectra of two sets of samples is revealed in the dependence of the intensity of narrow "substrate" band at 520 cm^{-1} on annealing temperature (*Fig. 1*). Usually, the light scattering from Si substrate is an undesirable obstacle in the RS measurements of SRSN films. The strong signal from bulk crystalline Si at 520 cm^{-1} prevents the observation of weak bands of amorphous and crystalline precipitates in the region of (450 – 520 cm^{-1}). Though, one can get useful information on phase composition of the nitride films from the analysis of "substrate" peak intensity when the annealing temperature increases. It can be seen in *Fig. 2* where the intensity of "substrate" band as a function of the annealing

temperature for the both sets of samples is presented. The intensity of this band increases significantly after the annealing at 1200 °C for both samples $SiN_{0.46}$ and $SiN_{1.0}$. It can be explained by the restoration of host silicon nitride matrix via the annealing of structural defects. On the other hand, the crystallization of Si clusters can result in the increase of intensity at 520 cm^{-1}, too. The inset in *Fig. 2* shows the absorption spectra of crystalline and amorphous silicon adopted from Ref. [41]. The vertical line at 473 nm in the inset indicates the exciting laser line used in our RS measurements. As can be seen from *Fig. 2*, the absorption at 473 nm in amorphous Si is stronger than in crystalline Si. Therefore, the light transmittance of the SiN_x layer with crystalline Si clusters should be higher in comparison with the SiN_x layer contained amorphous clusters. It is obvious, if the top layer becomes more transparent, the registered light scattering from the substrate increases. Thus, the significant increase of the intensity of 520 cm^{-1} band after the annealing at 1200 °C can be explained by the crystallization of initial amorphous Si clusters in addition to the annealing of defects in the host silicon nitride matrix.

However, there is an obvious difference between two curves in *Fig. 2*. With the increase of annealing temperature to 1000 °C, the intensity of 520 cm^{-1} peak increases for the $SiN_{1.0}$ sample and decreases for the $SiN_{0.46}$ sample. It should be noted that the intensity of bands at 480 cm^{-1} originated from the amorphous Si clusters is similar for both as-deposited samples. One can suggest that the amount of excessive silicon aggregated in clusters is similar in both as-deposited samples. Though, the above-mentioned RBS data demonstrate a higher Si content for the $SiN_{0.46}$ sample in comparison with the $SiN_{1.0}$ sample. Hence, the amount of excess Si atoms distributed randomly in the SiN_x matrix is higher in the $SiN_{0.46}$ film. Volodin *et al*. [33] observed the increasing absorption of SiN_x (*x*<1) films in the range of 250 − 500 nm after the furnace annealing at 1130 °C for 5 h in Ar ambient. This increase of the SiN_x layer absorption was explained by the formation of amorphous Si clusters during annealing. In our case, similar process can occur in the film $SiN_{0.46}$ upon annealing at 800 − 1000 °C. Namely, the formation of amorphous clusters from excess silicon atoms distributed in the SiN_x matrix can result in

increase of SiN_x layer absorption, too. As a result, the transmittance of the top SiN_x layer and light scattering by the Si substrate should decrease. Taking into account that the average size of Si clusters in the $SiN_{0.46}$ sample is larger than in the $SiN_{1.0}$ sample, one can suppose that the clusters in the as-deposited sample $SiN_{0.46}$ are too large to be crystallized under annealing at a temperature of 800 - 1000°C. Thus, an insufficiently high temperature for the crystallization of amorphous clusters and the formation of new amorphous Si clusters during the annealing at 800 – 1000 °C can result in decreasing the light scattering by the substrate for the sample $SiN_{0.46}$. On the contrary, the smaller clusters begin crystallize at a lower temperature in the $SiN_{1.0}$ sample, and the intensity of 520 cm^{-1} peak slowly increases with increasing annealing temperature in the range of 800 – 1000°C. It should be noted, when the low-energy tail of 520 cm^{-1} peak from silicon nanocrystals appears in the RS spectra (after annealing at 1200 and 1000 °C for $SiN_{0.46}$ and $SiN_{1.0}$ samples, respectively) the PL background is recorded in the range of 1500-3000 cm^{-1} (*Fig.1*). One can suggest that this PL arises from Si nanocrystals.

Figure *3*a shows the PL spectra of $SiN_{0.46}$ and $SiN_{1.0}$ samples annealed at 1200 °C for 3 min. These PL spectra can be deconvoluted into three fitted Gaussians. For the both samples, the blue-violet PL band at 440 nm is the most intensive one. Also, the red PL with maximum at ~640 nm is observed for both samples, but the PL spectrum of $SiN_{0.46}$ film is much more intense in the red region. Between these two bands there is a third one with different maximum positions for two samples. So, for $SiN_{0.46}$ film this band maximum is localized in the green range (at 510 nm) while for $SiN_{1.0}$ film it is found at 480 nm (in the blue range). It is reasonable to assume that different emission mechanisms are responsible for these PL bands.

Let us begin with the discussion of luminescence mechanism for the most intensive band at 440 nm. Over the past two decades, different native defect-related centers of radiative recombination in silicon nitride have been revealed and studied [28-29, 42-45]. Among of them the N-center is a two-fold coordinated nitrogen atom ($Si_2=N\bullet$). According to Desphande *et al.* [28], the presence of such defects can lead to light emission at 3 ± 0.1 eV. In Ref. [46] electron

spin resonance measurements reveal that N-centers may exist in the as-deposited films, but high temperature annealing (>700 °C) creates much more N-centers. In our case, the annealing at 1200 °C can result in the formation of N-centers. Thus, the PL band at 440 nm can be attributed to the radiative recombination of carriers at N-centers.

There is other native defect called K-center (a silicon atom bonded to three nitrogen atoms ($N_3\equiv Si\bullet$)) in silicon nitride. The presence of K-centers in silicon nitride matrix can result in green PL in the range of 2.5 ± 0.1 eV [28, 44]. In $SiN_{0.46}$ samples, the amount of excess silicon atoms distributed over the silicon nitride matrix, and avoiding clustering, is larger than in $SiN_{1.0}$ films. Hence, a high concentration of silicon dangling bonds (K-centers) is expected in $SiN_{0.46}$, and the green PL (510 nm) can be attributed to the K-centers, in this case.

As regarding a nature of the red PL band (640 nm) for $SiN_{0.46}$ sample and the blue band (480 nm) for $SiN_{1.0}$ sample, we ascribe them to emitting Si nanocrystals. The average size of silicon nanocrystals can be estimated from the position of first-order Raman peak using the following formula [20]:

$$L \cong \frac{\exp(-\pi^2)}{3} \cdot \frac{1}{[\omega_L - \omega_0]^2 + (\frac{\Gamma_0}{2})^2}, \tag{2}$$

where ω_L is the Raman frequency for silicon crystalline clusters of size L, and Γ_0 is the natural line width. For bulk crystal silicon ω_0 and Γ_0 amount to 520 and 3.5 cm^{-1}, respectively. In our case, it is difficult to determine the average diameter of silicon nanocrystals and size distribution by the Raman spectra due to a strong light scattering from the substrate. However, one can estimate that in the case of $SiN_{1.0}$ sample low-energy tail, ascribed to silicon nanocrystals, is stretching approximately from 508 to 514 cm^{-1} (*Fig. 3b)*. According to the equation (2), it originates from small crystals with size of ~1-4 nm. It means that the sample $SiN_{1.0}$ contains small silicon clusters with size <4 nm. For $SiN_{1.0}$ sample, the low-energy shoulder of the band at 520 cm^{-1} is more obvious and distinctive. In the case of $SiN_{0.46}$ film, this feature is almost negligible (nearly at the background level). It can be explained by the formation

of larger silicon nanocrystals (~4 nm and more) which do not lead to a noticeable Raman frequency shift. According to the quantum confinement effect, when the nanocrystal size reduces, the PL energy peak shifts toward the higher energy [26]. Hence, smaller Si nanocrystals in $SiN_{1.0}$ film should emit light in a more shortwave range in comparison with the larger ones in $SiN_{0.46}$ sample.

A schematic illustration of light emission mechanisms of two Si-rich SiN_x layers with different phase state of excessive Si in the nitride matrix is presented in *Fig. 4*. Annealing results in the formation of N-centers emitting light in the blue-violet range. The total Si content is higher for $SiN_{0.46}$ sample in comparison with that for $SiN_{1.0}$ sample. The heating at 1200 ℃ results in the aggregation of excessive Si in nanocrystals. The size of these nanocrystals reaches at least 4 nm and more for $SiN_{0.46}$ film while in the case of $SiN_{1.0}$ film it amounts to (1-4 nm). According to the quantum confinement effect, the smaller Si nanocrystals emit in the blue range ($SiN_{1.0}$ sample) and bigger ones emit in the red range ($SiN_{0.46}$ sample). We can also suggest that in the case of $SiN_{0.46}$ film some amount of excessive Si remains incorporated in nitride matrix not as Si nanocrystals, but as randomly distributed Si atoms in the atomic network. Such a scenario results in a high concentration of silicon dangling bonds (K-centers) and in the green PL.

4. Conclusions

We have studied the influence of annealing at (800 – 1200) °C on the phase transformation and light-emitting properties of two sets of SiN_x films denoted as $SiN_{0.46}$ and $SiN_{1.0}$. The films were deposited on Si wafers by low pressure chemical vapor deposition. The set $SiN_{0.46}$ is characterized by higher amount of excessive Si ($Si_{exc} \approx 26$ %) while for the set $SiN_{1.0}$ $Si_{exc} \approx 7$ %.

Amorphous Si clusters are revealed in as-deposited SiN_x films for both sets of samples. Annealing results in the formation of additional amorphous nanoclusters and in their crystallization with the increase of anneal temperature. Si nanocrystals are only revealed in nitride films of both sets after annealing at 1200 °C. Moreover, the nitride film with higher Si content ($SiN_{0.46}$) contains large silicon nanocrystals (~4 nm and more), and nitride film with

lower Si_{exc} ($SiN_{1.0}$) contains small silicon clusters with size <4 nm.

From the dependence of Raman scattering intensity for Si wafer on the temperature of annealing of SiN_x/Si structures and the RBS data, we can conclude that in the case of nitride films with higher Si content ($SiN_{0.46}$) some amount of excessive Si atoms are incorporated in nitride matrix as randomly distributed Si atoms in the atomic network, not as Si nanocrystals, even after annealing at 1200 °C. In the case of nitride film with lower excess of Si ($SiN_{1.0}$), practically all excessive Si atoms are aggregated into Si nanocrystals after annealing at 1200 °C.

Visible photoluminescence at the room temperature was detected for $SiN_{0.46}$ and $SiN_{1.0}$ samples annealed at 1200 °C. The blue-violet PL band at 440 nm is the most intensive one for both sets of the samples. Also the red PL at ~640 nm is observed for both samples, but the PL spectrum of $SiN_{0.46}$ sample is much more intense in the red region. Between these two bands there is a third one with different maximum positions for two samples (at 510 nm for $SiN_{0.46}$ and at 480 nm for $SiN_{1.0}$). The observed peculiarities of PL spectra for $SiN_{0.46}$ and $SiN_{1.0}$ films are explained taking into account a contribution from the quantum confinement effect on Si nanocrystals and from the native defects in silicon nitride matrix, such as N- centers ($Si_2=N\bullet$) and K-centers ($N_3\equiv Si\bullet$).

Acknowledgement

REFERENCES

1. J. G. Zhu, C. W. White, J. D. Budai, S. Y. Chen, P. Withrow, Growth of Ge, Si, and SiGe nanocrystals in SiO_2 matrices, J. Appl. Phys. 78 (1995) 4386-4389.

2.   O. Jambois, J. Carreras, A. Perez-Rodriguez, B. Garrido, C. Bonafos, S. Schamm, G. Ben Assayag, Field effect white and tunable electroluminescence from ion beam synthesized Si- and C-rich SiO$_2$ layers, Appl. Phys. Lett. 91 (2007) 211105.

3.   K. Ma, J. Y. Feng, Z. J. Zhang, Improved photoluminescence of silicon nanocrystals in silicon nitride prepared by ammonia sputtering, Nanotechnology 17 (2006) 4650-4653.

4.   X. Zeng, W. Liao, G. Wen, X. Wen, W. Zheng, Structural evolution and photoluminescence of annealed Si-rich nitride with Si quantum dots prepared by plasma enhanced chemical vapor deposition, Appl. Phys. Lett. 115 (2014) 154314.

5.   D. Hiller, A. Zeleninat, S. Gutsch, S. A. Dyakov, L. Lopez-Vidrier, S. Estrade, F.Peiro, B. Garrido, J. Valenta, M. Korinek, F.Trojanek, P. Maly, M. Schnabel, C. Weiss, S.Janz, and M. Zachrias, Absence of quantum confinement effects in the photoluminescence of Si$_3$N$_4$-embedded Si nanocrystals, J. Appl. Phys. 115 (2014) 204301.

6.   R. Chen, D. F. Qi, Y. J. Ruan, S. W. Pan, S. Y. Chen, S. Xie, C. Li, H. K. Lai, H. D. Sun, Effect of excimer laser annealing on the silicon nanocrystals embedded in silicon-rich silicon nitride film, Appl. Phys. A. 106 (2012) 251-255.

7.   M. D. Henry, S. Watavalkar, A. Homyk, A. Scherer, Alumina etch masks for fabrication of high-aspect-ratio silicon micropillars and nanopillars, Nanotechnology 20 (2009) 255305.

8.   S. S. Watavalkar, C. E. Hofman, A. P. Homyk, M. D. Henry, H. A. Aywater, A. Scherer, Tunable visible and near-IR emission from sub-10 nm etched single-crystal Si nanopillars, Nano Lett. 10 (2010) 4423-4428.

9.   N. Shin, M. A. Filler, Controlling silicon nanowire growth direction via surface chemistry, Nano Lett. 12 (2012) 2865-2870.

10. S. Ganguly, N. Kazem, D. Carter, S. M. Kauzlarich, Colloidal synthesis of an exotic phase of silicon: the BC8 structure, J. Am. Chem. Soc. 136 (2014) 1296-1299.

11. H. L. Hao, L. K. Wu, W. Z. Shena, H. F. W. Dekkers, Origin of visible luminescence in hydrogenated amorphous silicon nitride, Appl. Phys. Lett. 91 (2007) 201922.

12. Y. Q. Wang, Y. G. Wang, L. Cao, Z. X. Cao, High-effiency visible photoluminescence from amorphous silicon nanoparticles embedded in silicon nitride, Appl. Phys. Lett. 83 (2003) 3474-3476.

13. N. M. Park, T. S. Kim, S. J. Park, Band gap engineering of amorphous silicon quantum dots for light-emitting diodes, Appl. Phys. Lett. 78 (2001) 2575-2577.

14. A. Rodriguez, J. Arenas, J. C. Alonso, Photoluminescence mechanism in silicon quantum dots embedded in nanometric chlorinated-silicon nitride films, J. Lumin. 132 (2012) 2385-2389.

15. A. Marconnet, M. Panzer, S. Yerci, S. Minissale, X. Wang, X. Zhang, L. D. Negro, K. E. Goodson, Thermal conductivity and photoluminescence of light-emitting silicon nitride films, Appl. Phys. Lett. 100 (2012) 051908.

16. O. Debieu, R. P. Nalini, J. Cardin, X. Portier, J. Perriere, F. Gourbilleau, Structural and optical characterization of pure Si-rich nitride thin films, Nanoscale Res. Lett. 8 (2013) 31.

17. P. D. Nguen, D. M. Kepaptsoglou, Q. M. Rammasse, A. Olsen, Direct observation of quantum confinement of Si nanocrystals in Si-rich nitrides, Phys. Rev. B 85 (2012) 085315.

18. L. V. Mercaldo, E. M. Esposito, P. D. Veneri, B. Rezgui, A. Sibai, G. Bremond, Photoluminescence properties of partially phase separated silicon nitride films, J. Appl. Phys. 109 (2011) 093512.

19. J. Kistner, X. Chen, Y. Wenig, H. P. Strunk, M. B. Schubert, J. H. Werner, Photoluminescence from silicon nitride – no quantum effect, J. Appl. Phys. 110 (2011) 023520.

20. B. Sain, D. Das, Tunable photoluminescence from nc-Si/a-SiN$_x$:H quantum dot thin films prepared by ICP-CVD, Phys. Chem. Phys. 15 (2013) 3881-3888.

21. A. Rodiguez-Gomez, A. Garcia-Valenzuela, E. Haro-Poniatowski, Effect of thickness on the photoluminescence of silicon quantum dots embedded in silicon nitride films, J. Appl. Phys. 113 (2013) 233102.

22. J. C. Alonso, F. A. Pulgarin, B. M. Monroy, A. Benami, M. Bizarro, A. Ortiz, Visible electroluminescence from silicon nanoclusters embedded in chlorinated silicon nitride thin films, Thin Solid Films 518 (2010) 3891 – 3893.

23. Z. H. Cen, T. P. Chen, L. Ding, Y. Liu, J. I. Wong, M. Yang, Z. Liu, W. P. Goh, F. R. Zhu, S. Fung, Strong violet and green-yellow electroluminescence from silicon nitride thin films multiply implanted with Si ions, Appl. Phys. Lett. 94 (2009) 041102.

24. R. Huang, J. Song, X. Wang, Y. Q. Guo, C. Song, Z. H. Zheng, X. L. Wu, P. K. Chu, Origin of strong white electroluminescence from dense Si nanodots embedded in silicon nitride, Opt. Lett. 37 (2012) 692-694.

25. D. Li, F. Wang, D. Yang, Evolution of electroluminescence from silicon nitride light-emitting devices via nanostructurals silver, Nanoscale 5 (2013) 3435-3440.

26. T. W. Kim, C. H. Cho, B. H. Kim, S. J. Park, Quantum confinement effect in crystalline silicon quantum dots in silicon nitride grown using SiH_4 and NH_3, Appl. Phys. Lett. 88 (2006) 123102.

27. Y. H. So, S. Huang, G. Conibeer, M. A. Green, Formation and photoluminescence of Si nanocrystals in controlled multilayer structure comprising of Si-rich nitride and ultrathin silicon nitride barrier layers, Thin Solid Films 519 (2011) 5408-5412.

28. S. V. Desphande, E. Gulari, S. W. Brown, S. C. Rand, Optical properties of silicon nitride films deposited by hot filament chemical vapor deposition, J. Appl. Phys. 77 (1995) 6534-6541.

29. M. Wang, D. Li, Z. Yuan, D. Yang, D. Quen, Photoluminescence of Si-rich silicon nitride defect-related states and silicon nanoclusters, Appl. Phys. Lett. 90 (2007) 131903.

30. L. D. Negro, J. H. Yi, J. Michail, L. C. Kimerling, T. W. F. Chang, V. Sukhovatkin, E. H. Sargent, Light emission efficiency and dynamics in silicon-rich silicon nitride films, Appl. Phys. Lett. 88 (2006) 233109.

31. B. C. Joshi, G. Eranna, D. P. Runthala, B. B. Dixit, O. P. Washawan, P. D. Vyas, LPCVD and PECVD silicon nitride for microelectronics technology, Indian J. Eng. Mater. S. 7 (2000) 303-309.

32. D. Benoit, P. Morin, J. Regolini, Determination of silicon nitride film chemical composition to study hydrogen desorption mechanism, Thin Solid Films 519 (2011) 6550-6553.

33. V. A. Volodin, K. O. Bugaev, A. K. Gutakovsky, L. I. Fedina, M. A. Neklyudova, A. V. Latyshev, A. Misiuk, Evolution of silicon nanoclusters and hydrogen in SiN_x:H films: Influence of high hydrostatic pressure under annealing, Thin solid films 520 (2012) 6207-6214.

34. P. Colomban, Raman analyses and "smart" imaging of nanophases and nanosized materials, Spectroscopy Europe 15 (2003) 8-15.

35. P. R. J. Wilson, T. Roschuk, K. Dunn, E. N. Normand, E. Chelomentsev, O. H. Y. Zalloum, J. Wojcik, P. Mascher, Effect of thermal treatment on the growth, structure and luminescence of nitride-passivated silicon nanoclusters, Nanoscale Res. Lett. 6 (2011) 168.

36. V. A. Gritsenko, Electronic structure of silicon nitride, Phys.-USP 55 (2012) 498-507.

37. T. T. Korchagina, V. A. Volodin, B. N. Chichkov, Formation and crystallization of silicon nanoclusters in SiN_x:H films using femtosecond pulsed laser annealings, Semiconductors 44 (2010) 1611-1616.

38. J. E. Smith, Jr., M. H. Brodsky, B. L. Crowder, M. I. Nathan, A. Pinczuk, Raman spectra of amorphous Si and related tetrahedrally bonded semiconductors, Phys. Rev. Lett. 26 (1971) 642-646.

39. D. Nesheva, C. Raptis, A. Perakis, I. Bineva, Z. Aneva, Z. Levi, S. Alexandrova, H. Hofmeister, Raman scattering and photoluminescence from Si nanoparticles in annealed SiO_x thin films, J. Appl. Phys. 92 (2002) 4678-4683.

40. M. Hirasawa, T. Orii, T. Seto, Size-dependent crystallization of Si nanoparticles, Appl. Phys. Lett. 88 (2006) 093119.

41. R. Dewan, S. Fischer, V. Benno M. Rochow, Y. Ozdemir, S. Hamraz, D. Knipp, Studying nanostructured nipple arrays of moth eye facets helps to design better thin film solar cells, Bioinspir. Biomim. 7 (2012) 016003.

42. J. Kanicki, W. L. Warren, Defects in amorphous hydrogenated silicon nitride films, J. Non-Cryst. Solids 164 (1993) 1055-1060.

43. W. L. Warren, J. Kanicki, E. H. Poindexter, Paramagnetic point defects in silicon nitride and silicon oxynitride thin films on silicon, Colloids Surfaes A: Physicochem. Eng. Aspects 115 (1996) 311-317.

44. W. L. Warren, J. Robertson, J. Kanicki, Si and N dangling bond creation in silicon nitride thin films, Appl. Phys. Lett. 63 (1993) 2685-2687.

45. C. Ko, J. Joo, M. Han, B. Y. Park, J. H. So, K. Park, Annealing effects on the photoluminescence of amorphous silicon nitride films, J. Korean Phys. Soc. 48 (2006) 1277-1280.

46. B. Yan, J. H. Dias da Silva, P. C. Taylor, Defect structure in nitrogen-rich amorphous silicon nitride films, J. Non-Cryst. Solids 227 (1998) 528-532.

List of Figure and Table captions

Table 1 – Characteristics of as-deposited SiN$_x$ films of SiN$_{0.46}$ and SiN$_{1.0}$ sets.

Figure 1. Raman spectra of as-deposited (curve 1) and annealed at 800 °C (curve 2), 1000 °C (curve 3) and 1200 °C (curve 4) samples SiN$_{0.46}$ (a) and SiN$_{1.0}$ (b).

Figure 2. RS intensity of the band at 520 cm^{-1} from Si substrate as a function of annealing temperature for SiN$_{0.46}$ (curve 1) and SiN$_{1.0}$ (curve 2) sets. The inset shows the absorption spectra of the bulk crystalline and amorphous silicon from Ref. [41]. The vertical line indicates the exciting laser line in our RS measurements.

Figure 3. PL (a) and RS (b) spectra of SiN$_{0.46}$ (curve 1) and SiN$_{1.0}$ (curve 2) annealed at 1200 °C for 3 min. The dashed line represents the normalized spectrum of silicon substrate.

Figure 4. Schematic presentation of light-emitting sources in the sample SiN$_{0.46}$ (a) and SiN$_{1.0}$ (b). Color of halo around Si nanocrystals (grey spheres) corresponds to quantum confinement emission from Si nanocrystals: the red band (640 nm) for SiN$_{0.46}$ and the blue PL band (480 nm) for SiN$_{1.0}$. Insets are schematic images of silicon nitride luminescence defects (K- and N-centers)

Table 1

Samples	Refractive index n	Thickness, nm	Parameter x	Excess Si content Si_{exc}, %
$SiN_{0.46}$	2.2	850	0.46	26
$SiN_{1.0}$	2.2	950	1.00	7
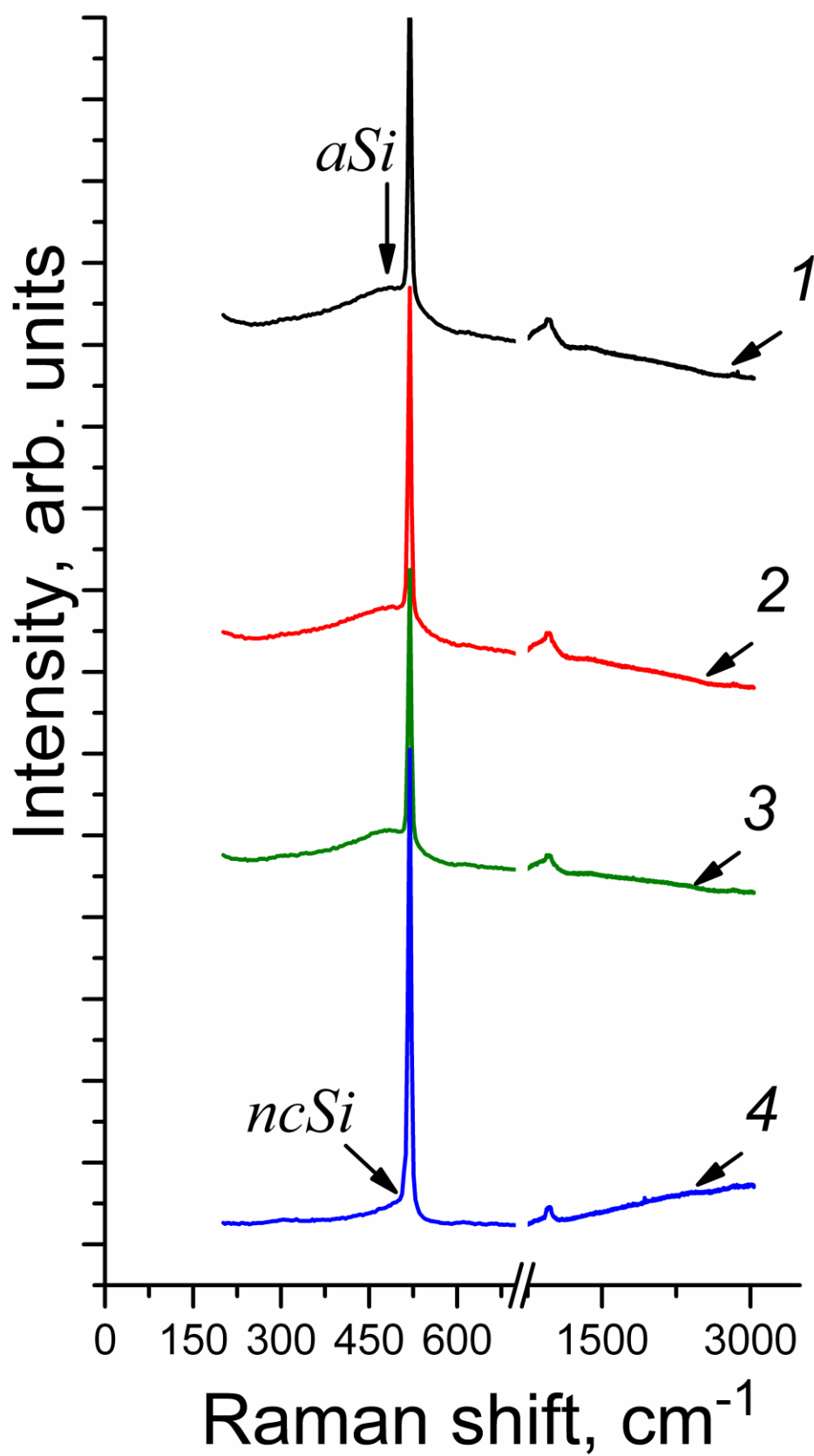
Figure 1a
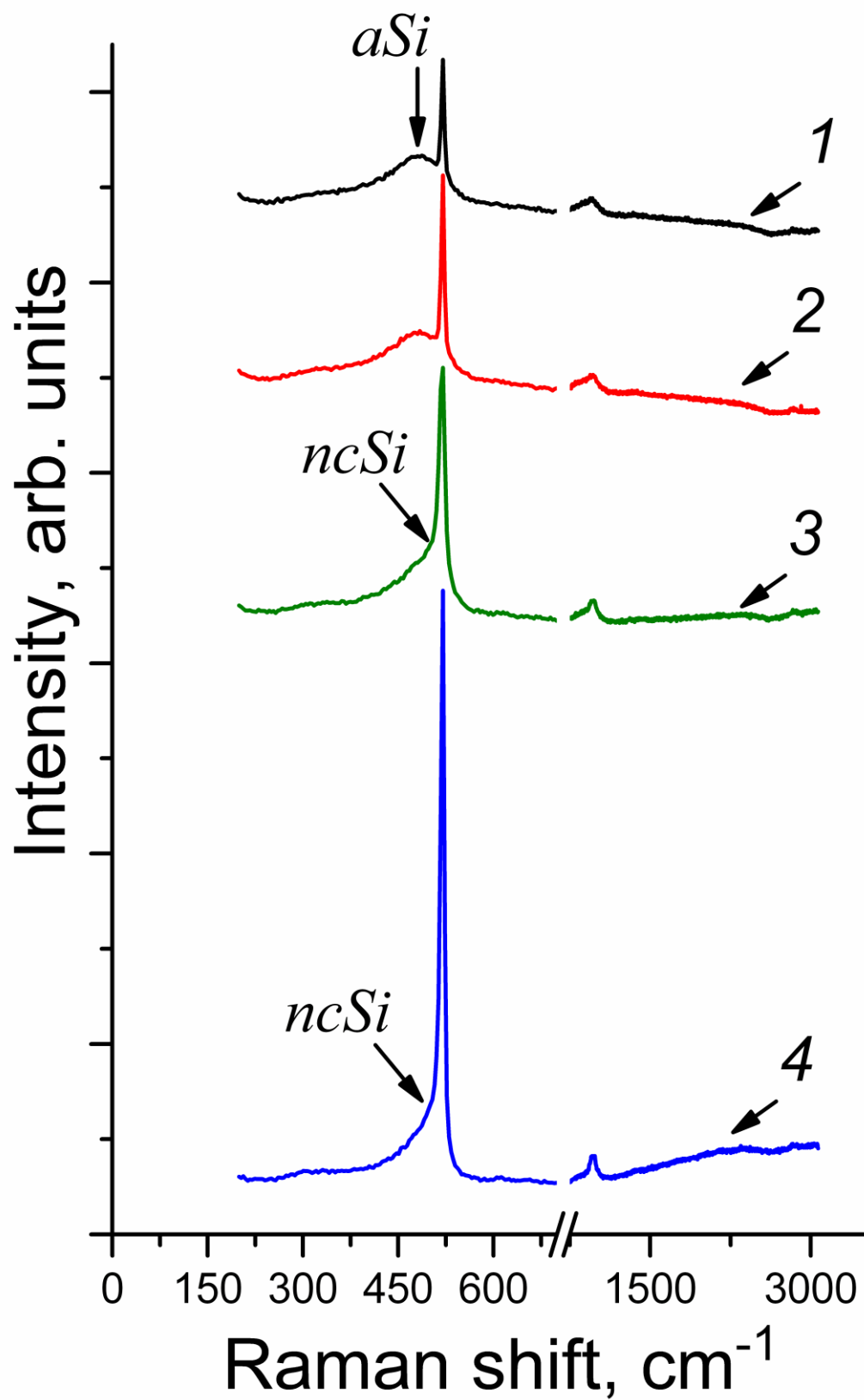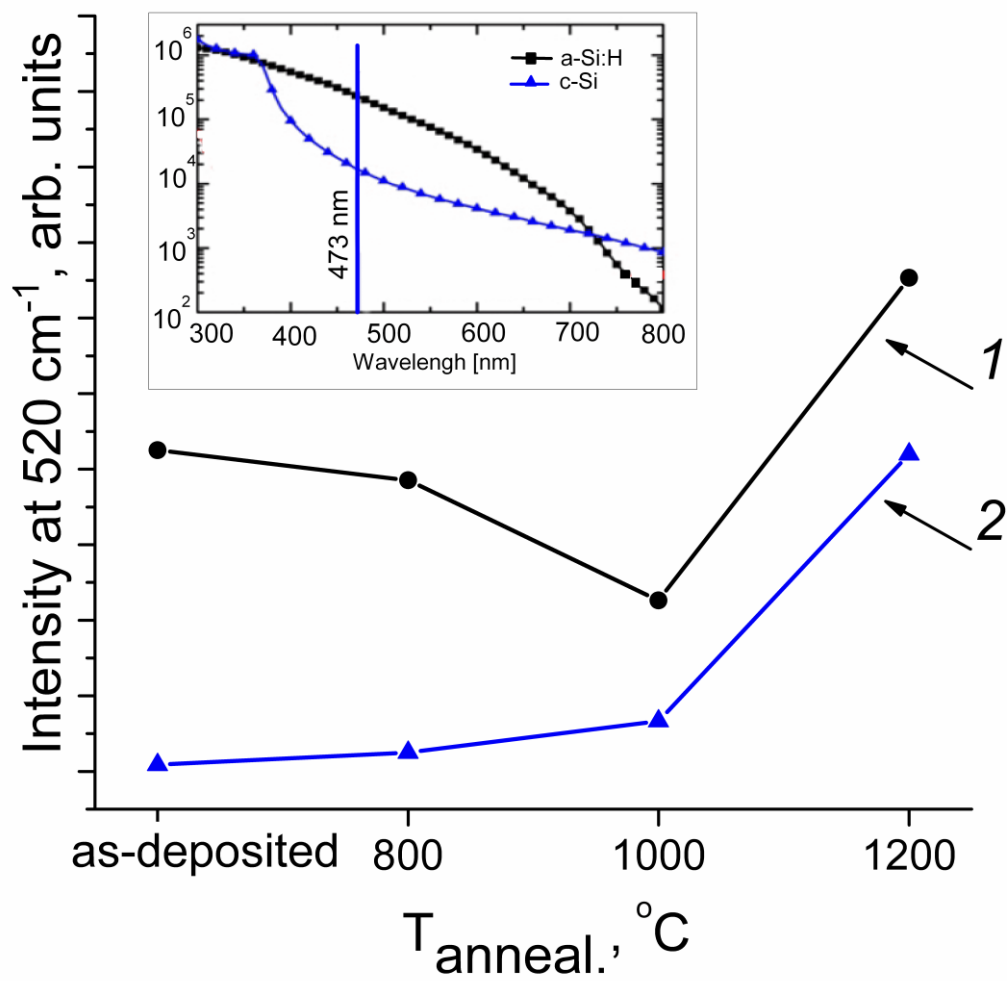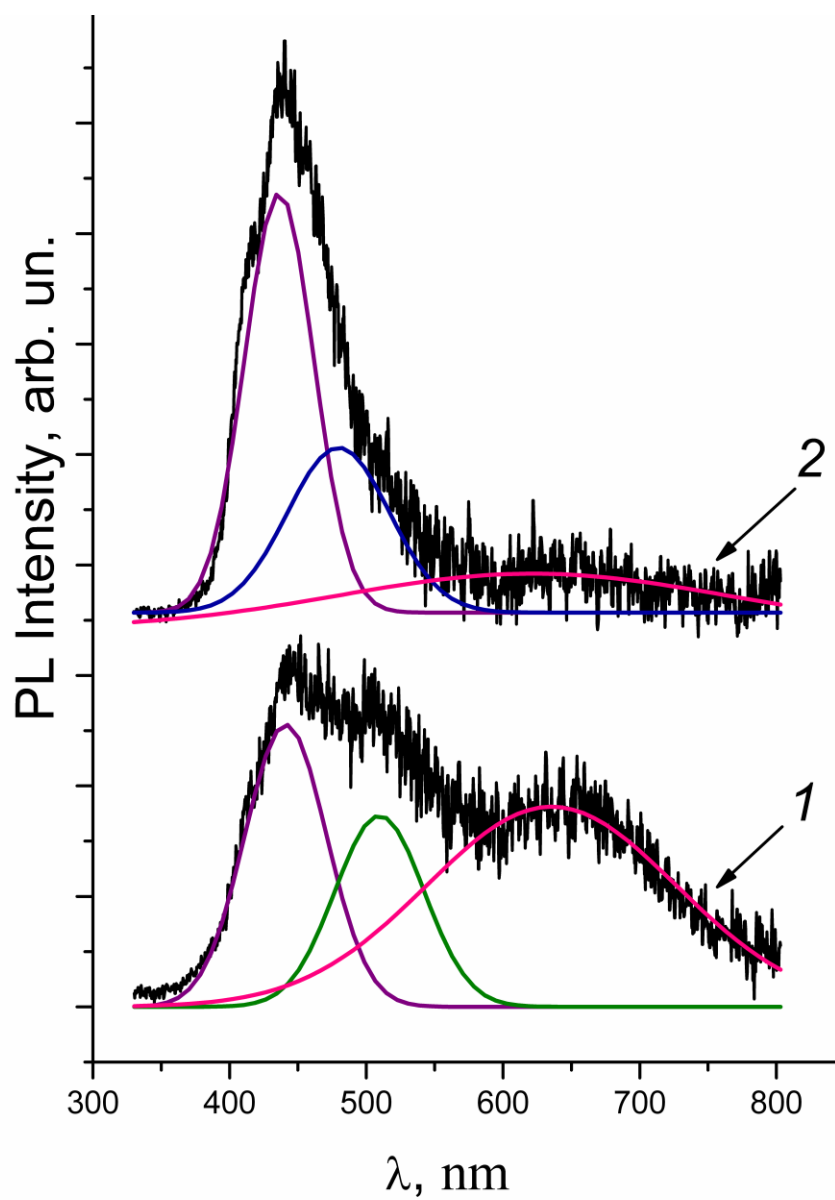
Figure 1b

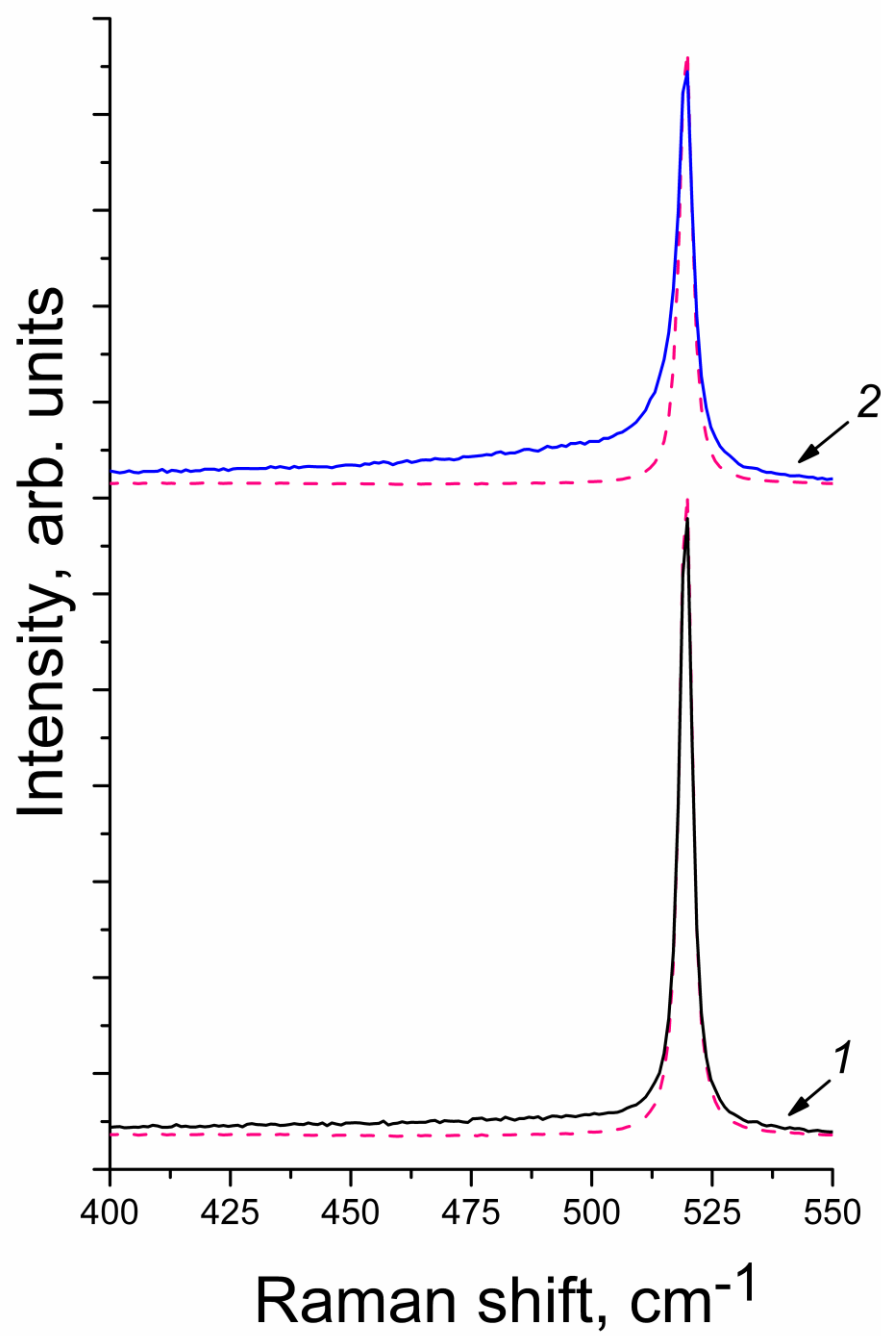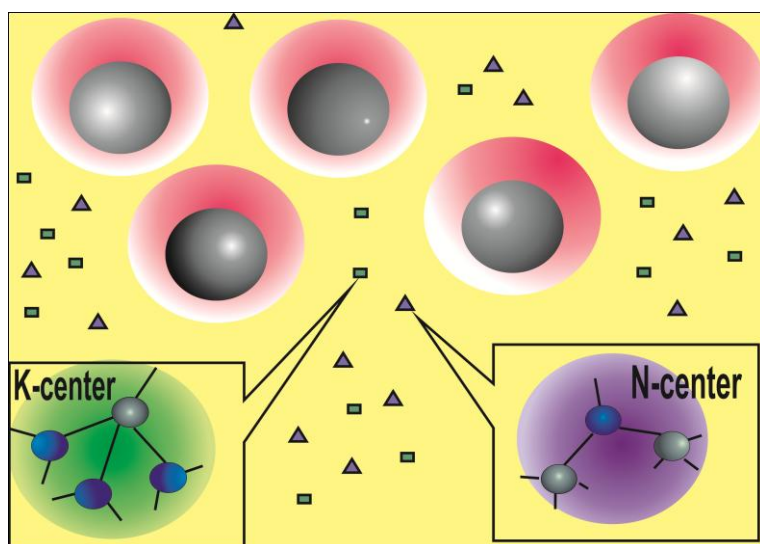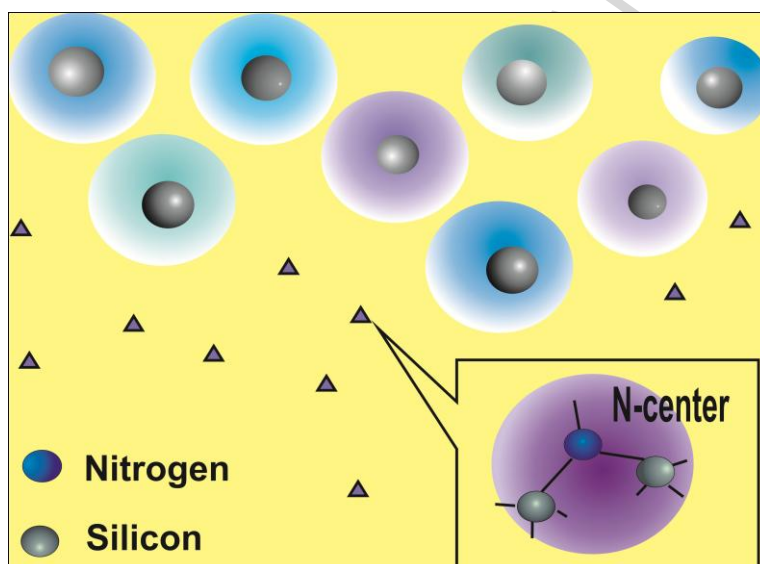**Figure 2**

A

B

Figure 3

A

B

Figure 4

Highlights

► The size of Si nanocrystals in Si-rich SiN_x films depends on Si excess content.

► Excess Si remains in $SiN_{0.46}$ as randomly distributed Si atoms in atomic network.

► In SiN_1 films practically all excess Si is aggregated into Si nanoclusters.